Self-Similarity and helical symmetry in vortex generator flow simulations

2014 J. Phys.: Conf. Ser. 555 012036

(http://iopscience.iop.org/1742-6596/555/1/012036)

Self-Similarity and helical symmetry in vortex generator flow simulations

U. Fernández[1], Clara M. Velte[2] P.-E. Réthoré[3] and N. N. Sørensen[3]

[1]Nuclear Engineering and Fluid Mechanics Department, University of the Basque Country, Nieves Cano 12, 01006 Vitoria-Gasteiz, Araba, Spain.

[2]Section of Fluid Mechanics, Department of Wind Energy, Technical University of Denmark, Nils Koppels Allé, 2800 Kgs. Lyngby, Denmark.

[3]DTU Wind Energy Division, Technical University of Denmark, Risø Campus, Bldg 115, Frederiksborgvej 399, DK-4000 Roskilde, Denmark.

E-mail: unai.fernandez@ehu.es

Abstract. According to experimental observations, the vortices generated by vortex generators have previously been observed to be self-similar for both the axial (u_z) and azimuthal (u_θ) velocity profiles. Further, the measured vortices have been observed to obey the criteria for helical symmetry. This is a powerful result, since it reduces the highly complex flow to merely four parameters. In the present work, corresponding computer simulations using Reynolds-Averaged Navier-Stokes equations have been carried out and compared to the experimental observations. The main objective of this study is to investigate how well the simulations can reproduce the physics of the flow and if the same analytical model can be applied. Using this model, parametric studies can be significantly reduced and, further, reliable simulations can substantially reduce the costs of the parametric studies themselves.

1. Introduction

Vortex Generators (VG) have been investigated for more than fifty years in applied aerodynamics on airplane wings, Taylor [1] and Wentz [2]. VGs are passive devices for flow control that enhance mixing of the boundary layer and can thus transfer high momentum fluid closer to the wall and thereby suppress separation, Rao et al. [3]. Figure 1 shows an artistic interpretation of the large scale flow mechanisms involved. They are frequently employed on wind turbine blades to enable the use of more slender blades. That is, one can reduce the width of a blade and thus also reduce weight for the same load distribution and power production. These devices are commonly triangular or rectangular vanes inclined at an angle to the incoming flow. These generators are usually dimensioned in relation to the local boundary layer thickness to obtain optimal interaction between the vortex and boundary layer, and are commonly placed in cascades in groups of two or more upstream of the flow separation area, Anderson [4].

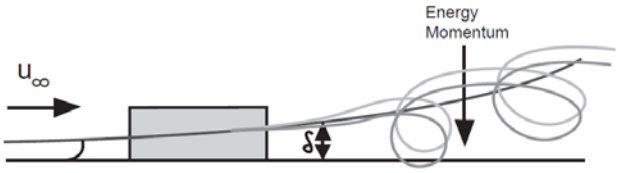

Figure 1: Boundary layer motion alteration by a rectangular VG.

Basic research on Vortex Generators mounted on a flat plate has previously occupied several researchers, see e.g. Lin [5]. For an example of successful control of a laminar separation bubble with significant drag reduction, see the investigations at moderate Reynolds number made by Kerho et al. [6]. Also Lin [5] observed the Drag reducing and Lift increasing effects of micro VGs. Wendt [7] investigated an array of VG experimentally where the VGs were aligned to generate counter-rotating vortices.

On wind turbine blades VGs are in fact applied with two aims: to delay or prevent separation of the flow and to decrease the roughness sensitivity of the blade. They are usually mounted in a spanwise array on the suction side of the blade and have the advantage that they can be added as a post-production fix to blades that do not perform as expected. Vortex Generators extend the lift curve by suppressing turbulent separation through mixing of the outer flow of the airfoil with the boundary layer. The delay of turbulent separation leads to higher maximum lift values and increased stall angles. An overview of different airfoils with several VG options is listed in van Rooij and Timmer [8]. Adding VGs to wind turbine blades is a simple solution to improving the performance of a rotor, Schubauer et al. [9] and Bragg et al. [10].

The effect of VGs on a 1MW Wind Turbine was investigated by Øye [11], comparing the measured power curves on a wind turbine with and without VGs. The study showed that in the investigated case the VGs on average increased the output power for nearly all wind speeds.

Many models for the generated vortices have been presented over the years. Theoretical models include, e.g., the one by Smith [12] and a model presented by Velte et al. [13] that was developed and applied to show the helical symmetry of the vortices generated by a passive rectangular vane-type vortex generator. As for models incorporated into codes, most are variants of the practical BAY-model by Bender et al. [14], which introduces body forces using source terms in the Navier-Stokes equations to simulate the presence of a vane.

Self-similarity is a state of self-preservation across scales. For jets and wakes this classically means that the development of the streamwise velocity profiles in the streamwise direction collapse for all positions if scaled correctly according to the theory presented, e.g., by White [15]. Figure 2(a) illustrates the wake velocity profile of a single VG on a flat plate at a distance d from the trailing edge of the vane, where U_∞ is the free stream velocity and u_0 the convection velocity (x and y represent the characteristic velocity scale and the characteristic shear-layer width respectively). The development of the axial velocity profiles downstream the VG is shown in figure 2(b) where the self-similarity concept is roughly sketched based on the idea of self-preservation across scales, White [15] and Crespo [16].

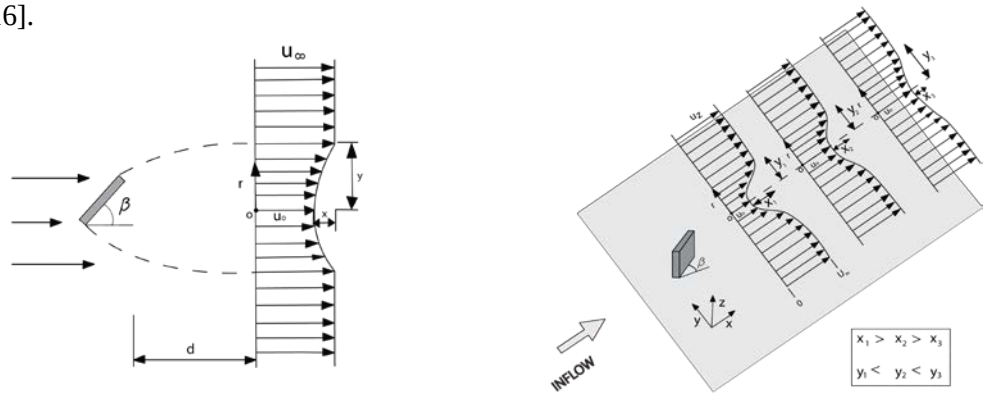

Figure 2: VG wake profiles. (a) Wake from a single VG and (b) development of the wake illustrated by streamwise velocity profiles.

As previously mentioned, Velte et al. [13] showed that the vortices produced by vortex generators possess helical symmetry. This means, in effect, that the streamwise (u_z), along the longitudinal vortex axis and the rotational (u_Θ) flows are inter-related by a simple linear relation based on the helical shape of the vorticity lines [13,17].

Previous experimental work by Velte [18] examines the downstream vortex evolution behind a cascade of vortex generators producing counter-rotating vortices in a boundary layer of negligible streamwise pressure gradient. The model parameters are all seen to vary linearly in the downstream direction. Based on the experimental observations triggered by a previous study [13], the vortices generated by vortex generators have been observed to be self-similar for both the axial (u_z) and azimuthal (u_Θ) velocity profiles. The previous model, which is based merely on u_z and u_Θ at one single downstream location, can therefore be extended to include the full downstream evolution of the developed part of the vortex using self-similarity scaling arguments. This knowledge is important for fundamental understanding as well as for the aspect of applications, for which parametric experiments can be substantially reduced in terms of required time and cost.

In the present study CFD simulations have been carried out by EllipSys3D CFD Code (Michelsen [19] and Sørensen [20]), and compared with a wind tunnel experiment, where a test case was performed over a single vane mounted on the test section wall in a low-speed wind tunnel.

The main objective of this article is to investigate how well the simulations can reproduce the physics of the flow and if the same analytical model can be applied. Using this model, parametric studies can be significantly reduced and, further, reliable simulations can substantially reduce the costs of the parametric studies themselves. For this purpose CFD simulations have been carried out and compared with a wind tunnel experiment and an analytical VG model.

2. Wind tunnel experiments

The experimental setup is the same as in Velte [18]. The experiments were conducted in a low-Reynold-number flow (Re=2600 based on an inlet turbulence-generating grid size L=39mm and free stream velocity U_∞ = 1.0 ms^{-1}). The wind tunnel speed was obtained by measuring the pressure drop across an orifice plate. The turbulence intensity at the inlet from laser doppler anemometry (LDA) measurements has been found to be 13 %. The boundary layer thickness at the position of the vortex generators has been estimated from LDA measurements to be approximately δ_{VG} = 25 mm. The actuators were a rectangular vanes of the same height as the local boundary layer thickness, $h = \delta_{VG}$, with a length of *2h*.

The measurements were conducted in spanwise planes, with planes normal to the test section wall, positioned in different positions downstream of the vortex generators. The SPIV equipment was mounted on a rigid stand and included a double cavity New Wave Solo 120XT Nd-YAG laser (wavelength 532 nm) capable of delivering light pulses of 120 mJ. The pulse width, i.e., the duration of each illumination pulse, was 10 ns. The light-sheet thickness at the measurement position was 2 mm and was created using a combination of a spherical convex and a cylindrical concave lens. The equipment also included two Dantec Dynamics Hi-Sense MkII cameras (1344 ×1024 pixels) equipped with 60 mm lenses and filters designed to only pass light with wavelengths close to that of the laser light.

3. Computational configuration.

In the present work, steady state simulations have been carried out and compared to the experimental observations. These computations were performed using the EllipSys3D code, see Michelsen [19] and Sørensen [20]. This in house CFD (Computational Fluid Dynamics) code is a structured finite-volume flow solver using, in this work, Reynolds-Averaged Navier-Stokes equations. The pressure/velocity coupling is ensured using the SIMPLE algorithm. The convective terms are discretized utilising the third order Quadratic Upstream Interpolation for Convective Kinematics (QUICK), Khosla et al. [21].

For these computations the *k-ω SST* (Shear Stress Transport) turbulence model by Menter [22] was used.

The current setting consists of a single VG on a flat plate and the computational domain has been defined with the following dimensions, normalized with the VG height, as described in [23], figure 3.

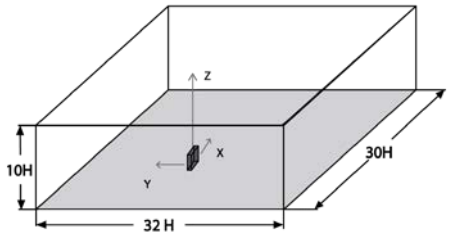

Figure 3: Computational domain

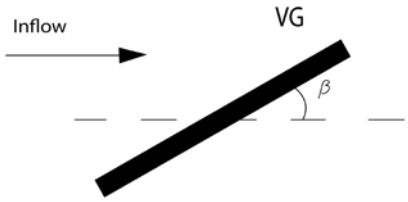

Figure 4: VG angle lay-out

The sketch represented in figure 4 illustrates the top view of the VG and shows that the thickness of the vane is constant. A boundary layer is developed across the test section floor, forced by the viscous interaction between the wall and the flow. The VG was positioned on a test section wall in such way that the boundary layer thickness at this location is equal to the VG height.

The angle of attack is β=20 degrees, figure 4, and the Reynolds Number based on VG height *H* is:

$$\mathrm{Re} = \frac{\rho U_\infty H}{\mu} = 2500 \qquad (3.1)$$

where ρ is the density, μ the viscosity and U_∞ the free stream velocity. The computational setup of the CFD simulations consists of a block structured mesh of 18 million cells with the first cell height ($\Delta z/H$) of 1.5 10^{-6} normalized by the VG height. Around the VG geometry, the mesh has 5.10^6 cells, while the mesh downstream the VG for capturing the wake has approximately $2.5.10^6$ cells, see Figures 5(a, b). In order to resolve the boundary layer, cell clustering has been used close to the wall and the dimensionless distance from the wall is less than 2 ($y^+<2$), as is required by the SST turbulence model.

Verification of sufficient mesh resolution was performed by a mesh dependency study. Results obtained for the finer mesh (66 blocks of 64^3 cells) are compared with results obtained for a standard (66 blocks of 32^3 cells) and a coarser mesh (66 blocks of 16^3 cells). The deviation between level-1 and level-2 indicates a difference of ~5% in the axial velocity.

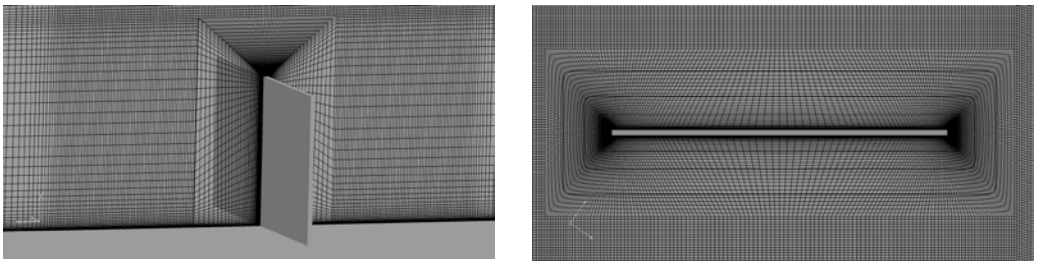

Figure 5: Mesh Sections on the VG. (a) Cross flow section and (b) top view.

The measurements in the computational simulations have been conducted in 5 spanwise planes, normal to the test section floor, located 5, 7.5, 10, 12.5 and 15 VG heights downstream of the vortex generator trailing edge when the angle of the device is zero, see figure 6.

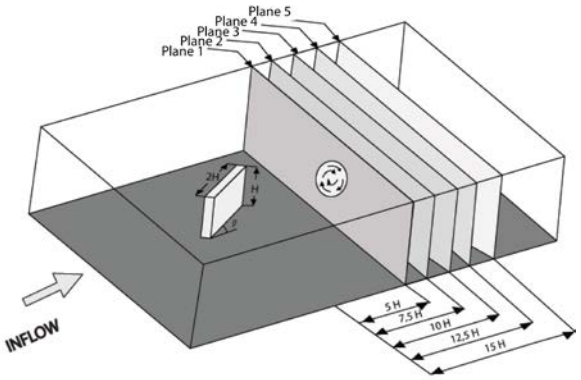

Figure 6: Plane location where the measurements were conducted.

4. Analytical model.

Only a brief description is given in the current text. For more details, please refer to [13, 18]. It has previously been shown that the generated vortices possess helical symmetry [13]. This means that the axial, u_z, and rotational, u_Θ, velocities are linearly related:

$$u_z = u_0 - r u_\theta / l \tag{4.1}$$

(z,Θ,r) are the coordinates in a polar coordinate system of the longitudinal vortex where z is along the vortex center axis. u_0 is the vortex convection velocity, r the radial coordinate and l the helical pitch. Together with the Batchelor vortex model

$$u_\theta(r,\theta,z) = \frac{\Gamma(z)}{2\pi r}\left[1-\exp\left(-\frac{r^2}{\varepsilon^2(\theta,z)}\right)\right]; \quad u_z(r,\theta,z) = u_0(z) - \frac{\Gamma(z)}{2\pi l(\theta,z)}\left[1-\exp\left(-\frac{r^2}{\varepsilon^2(\theta,z)}\right)\right] \tag{4.2}$$

this allows the generated flow to be described by merely four parameters: vortex core radius $\varepsilon(\Theta,z)$, circulation $\Gamma(z)$, convection velocity $u_0(z)$ and helical pitch $l(\Theta,z)$, leaving no restrictions on the shape of the vortex core. This model was further expanded to include the downstream vortex development using self-similarity analysis [18] in a low Reynolds number flow with a negligible streamwise pressure gradient. Self-similarity is based on the idea of self-preservation across scales. This kind of analysis is common for jets, but can conveniently be applied to wakes as well [15]. For the measured time-averaged far wake behavior it is posed that:

$$\frac{u_z - u_0}{U_e - u_0} = fcn\left(\frac{r}{\varepsilon}\right) \tag{4.3}$$

where the vortex core radius $\varepsilon(\Theta,z)$ is chosen as the characteristic width of the wake and U_e is the ambient streamwise velocity. Note that $\varepsilon=\varepsilon(\Theta,z)$, $l=l(\Theta,z)$ and $u_0= u_0(z)$ are all functions of the vortex axial coordinate z. The self-similarity relation (4.3) should also be compared to the velocity formulation, which has been confirmed to apply to the current flow [13], where the left-hand-side corresponds to the left-hand-side numerator in (4.3). A convenient scaling for the azimuthal velocity u_Θ is to normalize it by the maximum value of u_Θ. From self-similarity of both u_z and u_Θ, the model presented in [18] can be extended to include the downstream development (z-dependence) of the vortices. In practice, this model can therefore significantly reduce costly and time consuming parametric studies on vortex generators in future studies.

5. Testing of helical symmetry

The analysis of the helical symmetry was performed based on the computational results extracted in the cross planes positioned at z/h = 5, 7.5, 10, 12.5 and 15 VG heights downstream the trailing edge of the VG. Figure 7 illustrates the axial and azimuthal velocity profiles (upper values are the axial velocity profile u_z and lower the azimuthal one $u_{\theta.}$) for each plane position and are compared to the right-hand side of (4.1) calculated using the computational values u_θ (o). The two data sets overlap reasonably well for all plane positions and the variation between the CFD results and the axial velocity calculated by (4.1) is hardly visible. Note that the analysis has been carried out only on the right side, since a perturbing secondary vortex appears on the left side [13].

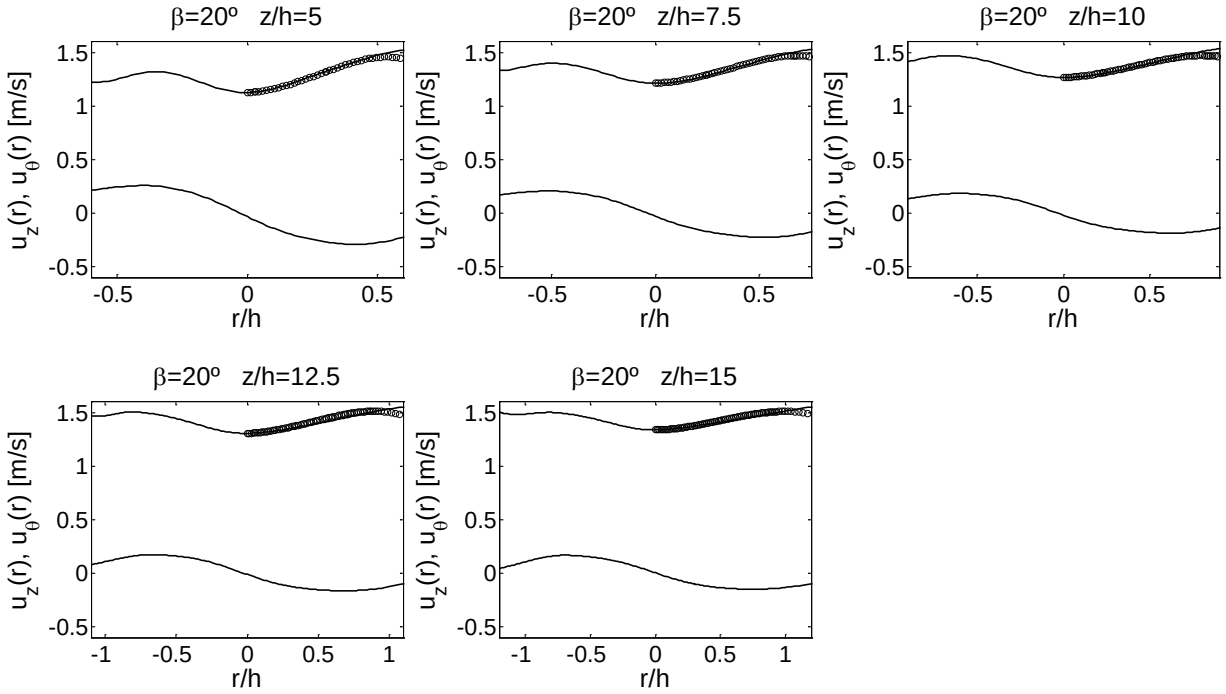

Figure 7: CFD velocity profiles of embedded vortices generated by a VG for a device angle β=20º. Upper values are the axial velocity profile u_z and lower the azimuthal one $u_{\theta.}$ CFD values of u_z are compared to the right-hand side of (4.1) calculated using the computational values u_θ (o).

6. Testing of wake self-similarity.

An angle of attack β =20º of the VG to the incoming flow was chosen for the computations and subsequently compared with the wind tunnel experiments and an analytical model as described in [18]. The extraction of velocities from the computations was conducted similar to the experimental procedure as in [13], in planes normal to the section wall downstream of the VG. The three velocity components were extracted along a line parallel to the wall passing through the center of the primary vortex.

Figures 8 and 9 displays the axial (u_z) and azimuthal (u_θ) velocity profiles of the wind tunnel and computational data respectively. Note that the left side of the plots, in particular for the axial velocity, a perturbation appears caused by a secondary vortex appearing due to the proximity of the primary vortex to the wall [13]. Figures 8 and 9 show that applying similarity scaling to both the u_z and u_θ profiles makes the curves collapse. Figures 9 shows the corresponding plots of the CFD velocity profiles of the vortex generated downstream the trailing edge of the VG at five plane positions z/h=5-15 with the device angle of incidence β=20º. Since the axial and azimuthal velocities are observed to

be self-similar, it is expected that u_0 and l vary linearly along the downstream path, which is shown in figure 11.

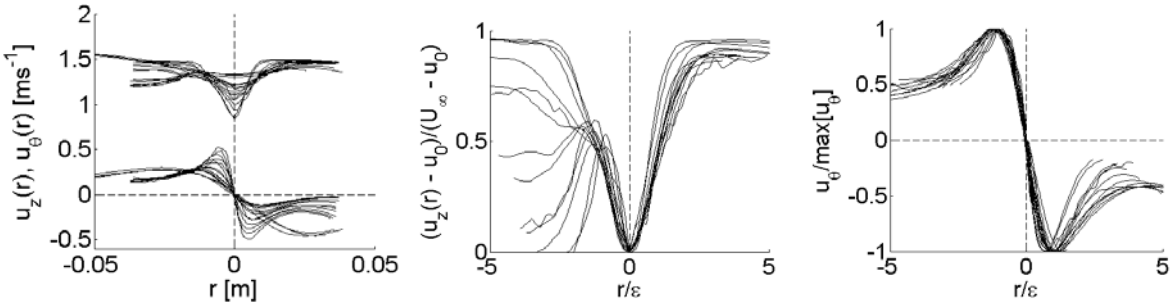

Figure 8: Velocity profiles from wind tunnel experiments for various angles and z/h = 2–13, showing the experimental values of the axial (u_z) and azimuthal (u_Θ) profiles (left column) and the axial (middle column) and azimuthal (right column) scaled by self-similarity variables.

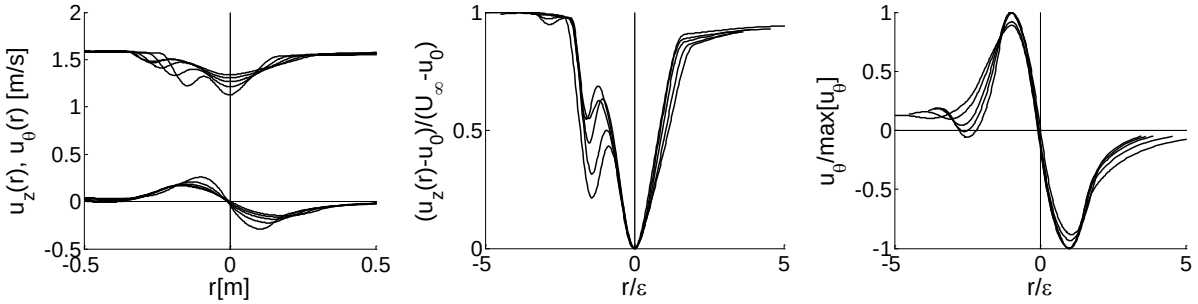

Figure 9: CFD velocity profiles at five plane positions z/h = 5-15. Left side shows the axial (u_z) and azimuthal (u_Θ) profiles and the middle and right sides show the axial and azimuthal profiles respectively, scaled by self-similarity variables.

Figures 10 and 11 display the stream-wise evolution of the helical parameters: vortex convection velocity (u_o), circulation through the vortex (Γ), helical pitch (l) and vortex core radius (ε) for the wind tunnel experiments and computational simulations respectively. The local flow characteristic u_o was found directly from the lowest value of the axial velocity wake profile and the helical pitch l was obtained from (4.1). The circulation has been calculated as the flux of vorticity across a surface enclosed by a curve described by the vortex radius. The vortex core radius ε has been obtained as the radius of the maximum value of the azimuthal velocity for each plane position. For a better comparison between the experimental and computational results, both vortex radius and helical pitch have been normalized by the VG height h. The convection velocity has been normalized by the free stream velocity U_∞ and the circulation by the multiplication of U_∞ and h.

According with [17], the negative sign of l represented in figures 10c and 11c indicates that the helical vortex has a left-hand symmetry. As expected, the only factor which does not vary along the plane positions is the circulation, which should be close to constant in a system of low viscous dissipation.

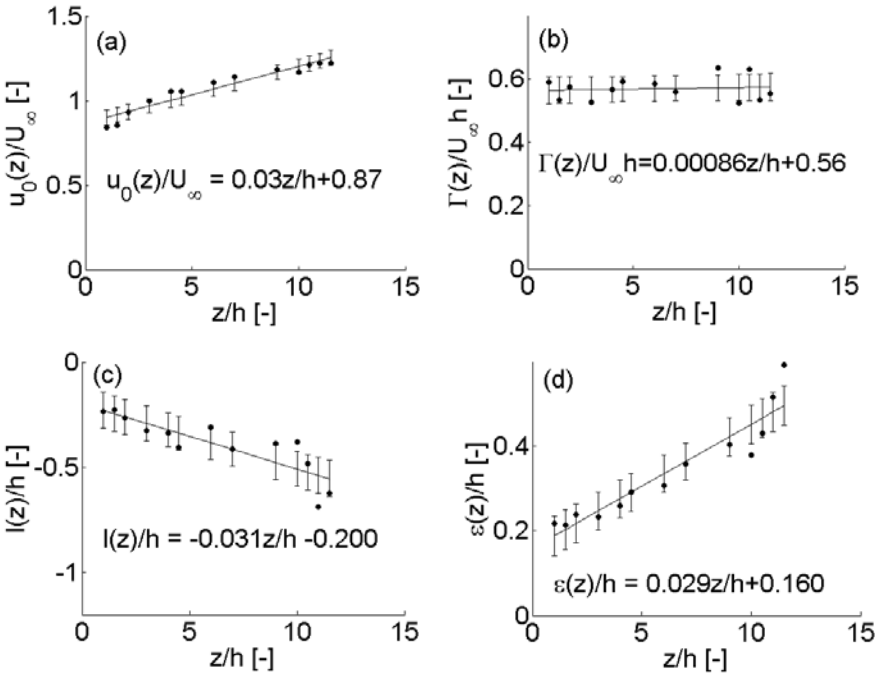

Figure 10: Experimental results of the downstream evolution of the characteristic vortex parameters in the stable wake.

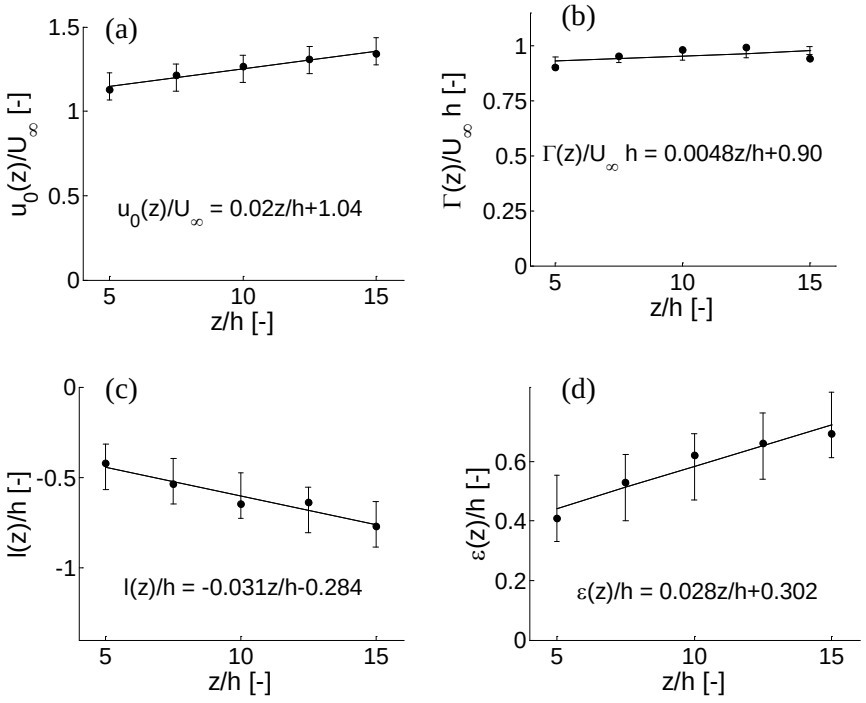

Figure 11: CFD results of the downstream evolution of the characteristic vortex parameters.

7. Conclusions.

In this article, vortices generated by a passive rectangular vane-type vortex generator of the same height as the boundary layer thickness in a test section wall have been studied. CFD computational simulations at Reynolds Number Re=2500 have been carried out using the RANS method and compared with wind tunnel experimental data and an analytical model.

The vortex generated by the VG shows self-similar behaviour for both the axial and azimuthal velocity profiles. It was proven based on five plane positions z/h=5, 7.5, 10, 12.5, 15 downstream of the trailing edge of the VG and with the angle of attack β=20º of the vane to the incoming flow. The CFD results represented in figure 9 show good agreement with the self-similarity shown in the experiments carried out in [18] and the trend of the entire characteristic vortex parameters in the computational results (figure 11) matches reasonably well the experimental observations (figure 10).

From the point of view of self-similarity, computational simulations are able to reproduce the physic of the vortex generated by a rectangular VG with considerable reliability. Also, the helical symmetry has been tested and verified based on the computational data.

For future investigations, it would be very interesting to achieve more computational simulations with different VG geometries and, also, of a row of VG's mounted on a bump.

Acknowledgements

The author is really grateful to the researcher E. Zulueta of the University College of Engineering Vitoria-Gasteiz (University of the Basque Country, Spain) for his helpful remarks. C.M. Velte and N.N. Sørensen were supported by EUDP-2009-II-Grant Journal No. 64009-0279, which is gratefully acknowledged.

References

[1] Taylor H D "Summary report on vortex generators". *Research Department Report No. R-05280-9.* United Aircraft Corporation, East Hartford, Connecticut, 1950.

[2] Wentz W H jr, "Effectiveness of spoilers on the GA(W)-1 airfoil with a high performance Fowler flap" *NASA CR-2538* May 1975.

[3] Rao D M, Kariya TT "Boundary-layer submerged vortex generators for separation control-an exploratory study". *AIAA Paper 88-3546-CP, AIAA/ASME/SIAM/APS 1st National Fluid Dynamics Congress*, Cincinnati, OH, July 25–28, 1988.

[4] Anderson B H, "The aerodynamic characteristics of vortex ingestion for the fla-18 inlet duct", NASA Lewis Research Center, Cleveland, Ohio 44135. *29th Aeroespace Sciences Meeting, Nevada*, January 1991.

[5] Lin J C "Review of research on low-profile vortex generators to control boundary layer separation". *Progress in Aerospace Sciences*, **Vol. 38**, No. 4–5, 2002, pp. 389–420.

[6] Kerho M, Huctcherson S, Blackwelder R F and R. H. Liebeck. "Vortex Generators used to control laminar separation bubbles". *Journal of Aircraft, **30**(3) 315-319*, 1993.

[7] Wendt B J "Parametric study of vortices shed from airfoil vortex generators". *AIAA Journal* **42**, 2185_2195, 2004.

[8] van Rooij R. P. J. O. M. and Timmer W A "Roughness Sensitivity Considerations for Thick Rotor Blade Airfoils". *AIAA-paper* 2003-0350.

[9] Schubauer G B and Spangenber W G "Forced mixing in boundary layers". *J Fluid Mech*, 1 1960;8:10–32.

[10] Bragg M B and Gregorek G M "Experimental study of airfoil performance with vortex generators". *Journal of aircraft*; **24**(5):305–9, 1987.

[11] Øye S "The Effect of Vortex Generators on the Performance of the ELKRAFT 1000 kW Turbine". *9th IEA Symposium on Aerodynamics of Wind Turbines*, Stockholm, Sweden, ISSN 0590_8809, 1995.

[12] Smith F T "Theoretical prediction and design for vortex generators in turbulent boundary layers," *J. Fluid Mech.*, **Vol. 270**, 1994, pp. 91–131.
[13] Velte C M, Hansen, M O L and Okulov V L "Helical structure of longitudinal vortices embedded in turbulent wall-bounded flow," *J. Fluid Mech.*, **Vol. 619**, 2009, pp. 167-177.
[14] Bender E E, Anderson B H and Yagle P J "Vortex Generator Modeling for Navier-Stokes Codes", *Proc. 3rd ASME/JSME Joint Fluids Engineering Conference*, San Francisco, California, USA, 1999.
[15] White F M Viscous Flow, 2nd ed., McGraw-Hill, Singapore, 1991, pp. 470-481.
[16] Crespo, A., Mecánica de Fluidos, Thomson Editores, Madrid, 2006, pp 685-707.
[17] Alekseenko S V, Kuibin P A and Okulov V L *Theory of Concentrated Vortices – An Introduction*, 1st ed., Springer-Verlag, Berlin Heidelberg, 2007, Chap. 1.
[18] Velte C M "A Vortex Generator Flow Model Based on Self-Similarity," *AIAA J., accepted for publication.*
[19] Michelsen J A "Basis3d- a platform for development of multiblock pde solvers". *Technical Report AFM 94-06*, Technical University of Denmark, Dept. of Mechanical Engineering, 1994.
[20] Sørensen N N "General purpose flow solver applied to flow over hills". Technical Report Risoe-*R-827(EN)*, Risoe National Laboratory, 1995.
[21] Khosla P K and Rubin S G "A diagonally dominant second-order accurate implicit scheme", *Computer Fluids*, **207-209**, 1974.
[22] Menter F R "Zonal Two equation k-ω Turbulence Model for aerodynamic flows", *AIAA Journal* 932906, 1993.
[23] Fernández U, Réthoté P-E, Sørensen N N, Velte C M, Zahle F and Egusquiza E "Comparison of Four Different Models of Vortex Generators", *Proceedings of EWEA* 2012.